Radiophysics and Quantum Electronics, Vol. 56, Nos. 8–9, January, 2014
(Russian Original Vol. 56, Nos. 8–9, August–September, 2013)

PRECISION SUB-DOPPLER MILLIMETER AND SUBMILLIMETER LAMB-DIP SPECTROMETER

G. Yu. Golubiatnikov,[1] * S. P. Belov,[1] I. I. Leonov,[1]
A. F. Andriyanov,[1] I. I. Zinchenko,[1] A. V. Lapinov,[1]
V. N. Markov,[1] A. P. Shkaev,[1] and A. Guarnieri[2]

UDC 535.343.4+535-14+544.17

We describe a precision sub-Doppler millimeter and submillimeter-wave Lamb-dip spectrometer with a backward-wave oscillator as the radiation source. The effect of nonlinear saturation of the spectral transitions (the Lamb-dip method) is used. The spectrometer resolution (about 5–10 *kHz) and the measurement accuracy of the absolute frequencies (of the order of* 1 *kHz) of molecular transitions in the frequency range below* 0.5 *THz are discussed. The spectrometer is designed for obtaining accurate radio-astronomy and molecular-spectroscopy experimental data, in particular, when seeking variation in the proton-to-electron mass ratio as a function of time and place in the Universe. The frequency records of the Lamb dips on the spectral lines of the* CO*, OCS, and* H_2O *molecules, the results of measuring the center frequencies of some transitions, and comparison with the results of other works are presented. The high measurement accuracy allows us to use the molecular-transition frequencies as the secondary frequency standards.*

1. INTRODUCTION

Nowadays it is necessary to obtain precision frequencies of molecular transitions and study their hyperfine structure for using them in the ground-based and space radio astronomy, as well as fundamental astrophysical and spectroscopic studies [1, 2].

The relatively simple method of nonlinear coherent spectroscopy, which is based on the line-saturation effect (the Lamb-dip method [3–5]), has some advantages and allows one to obtain a narrow nonlinear resonance inside the Doppler profile of the spectral line and measure its frequency with high accuracy in a wide frequency range at room temperature. The Lamb dip is usually an order of magnitude narrower than the Doppler linewidth in the millimeter- and submillimeter-wave ranges, which allows one to significantly improve the measurement accuracy of the center frequency of the line. In addition, in some cases, this method also allows one to measure the hyperfine structure of the lines, which is stipulated by the quadrupole, spin-rotational, and spin–spin interactions and is not resolved because of the Doppler broadening in a conventional spectrometer.

The measurements using the Lamb-dip method were among the first ones in the millimeter- and submillimiter-wave ranges in the resonator spectrometers for the OCS-molecule line with a width of about 1 kHz [6] near the frequency 36 GHz and for the water (H_2O)-molecule line at a frequency of 183 GHz [7]. Later, the exact secondary frequency standards for the radio-astronomy measurements on the basis of the frequency atlas of the rotational transitions of the $^{12}C\,^{16}O$ [8], $^{12}C\,^{18}O$ [9], OCS [10], HNCO [11], and H_2O [12] molecules in the millimeter- and submillimeter-wave ranges were developed.

* glb@ufp.appl.sci-nnov.ru

[1] Institute of Applied Physics of the Russian Academy of Sciences, Nizhny Novgorod, Russia; [2] Christian-Albrechts-Universität zu Kiel, Kiel, Germany. Translated from Izvestiya Vysshikh Uchebnykh Zavedenii, Radiofizika, Vol. 56, Nos. 8–9, pp. 666–677, August–September 2013. Original article submitted June 4, 2013; accepted September 30, 2013.

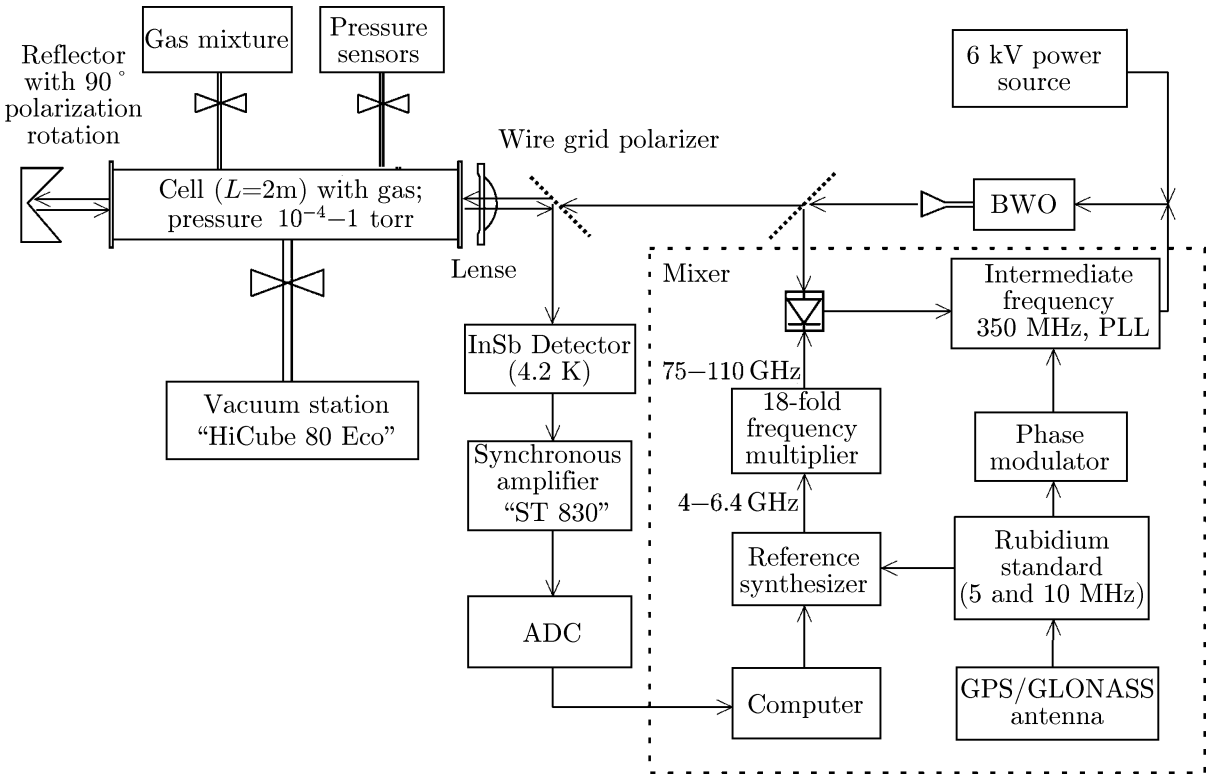

Fig. 1. Block diagram of the sub-Doppler wideband noncavity millimeter- and submillimeter-wave spectrometer with molecular-absorption saturation (Lamb dip) and the phase-stabilization system of the source BWO) Dots are used to denote the BWO phase-locked loop (PLL) and the frequency-control system.

Despite the advantages of the method, the nonlinear absorption character and the impossibility to visualize the distribution of the electromagnetic-beam field, i.e., insufficiently good reproducibility of the conditions of recording the spectral absorption lines, as well as some other factors which are considered below, do not make this method widely used in laboratory studies.

The wideband noncavity millimeter- and submillimeter-wave spectrometer, which uses the Lamb-dip method to obtain the narrow nonlinear resonances with a minimum width of up to 5–10 kHz inside the Doppler profile of the absorption lines of the rotational transitions of molecules and measure the frequencies of these lines with absolute accuracy better than 1 kHz, has been developed at the Institute of Applied Physics of the Russian Academy of Sciences (Nizhny Novgorod).

The spectrometer and its operation principles are described in this work along with the factors restricting the line-center measurement accuracy, spectral resolution, and sensitivity of the spectrometer. The examples of the measured spectral lines of the CO-, OCS-, and $H_2\,{}^{16}O$-molecule transitions are presented.

2. SPECTROMETER DESCRIPTION

The spectrometer operates as follows. A studied gas (or a gas mix) is injected up to the required pressure 10^{-4}–10^{-1} Torr into a spectrometer cell pre-evacuated to 10^{-6} Torr. The gas pressure is measured by an "MKS Baratron" membrane sensor (120AA and 626B models). A spectrometer cell is a 2 m long and 113 mm diameter stainless-steel tube with polished internal cell surface. Optical vacuum windows are made of high-density polyethylene and are cone-shaped to reduce the standing-wave amplitude between them.

A beam of the linear-polarized millimeter and submillimeter radiation, which is formed by a horn antenna and a lens, passes through a gas cell (Fig. 1), is reflected with the polarization-plane rotation by 90°, and is directed by a wire grid polarizer to the low-temperature ($T = 4.2$ K) bolometer or a semiconductor detector after the return passage through the cell. As the radiation passes through an absorbing gas layer

with thickness L, the radiation intensity decreases according to the exponential law $I(\nu) = I_\nu \exp[-\alpha(\nu)L]$, where I_ν is the incident-radiation intensity and $\alpha(\nu)$ is the absorption coefficient in gas at the frequency ν (Bouguer–Lambert–Beer law). The dependence of spectral-line profile $\alpha(\nu)$ on the radiation frequency is determined by the collisions of the absorbing molecules (Lorentz profile) and their thermal motion (Doppler profile), as well as the radiation intensity in the nonlinear case. In the sub-Doppler regime with the saturated populations of the molecular-transition levels by counterpropagating waves, a narrow Lamb dip whose width and depth depend on the gas pressure in the cell, energy-flux density, the relationship between the counterpropagating-wave intensities [13], and the radiation spectrum is formed at the top of the Doppler profile of the line. In the general case, the frequency profile of the Lamb dip can have a fairly complex shape and nonlinear dependence on the gas pressure and the radiation intensity [14]. In this work, the problem of determining the absorption-line frequency profile is not discussed.

A PTS-6400 frequency synthesizer (with the operation range 10–6400 MHz), along with the active circuit of frequency multiplication of the output signal by 18 (a multiplier– amplifier with a multiplication factor of 3, multiplier–amplifier with a frequency multiplication factor of 2, and a multiplier with a factor of 3), which was manufactured by the A. P. Gorshkov Research Institute of Electronic Measurements "KVARZ" (Nizhny Novgorod, Russia) was used as a tunable source of coherent radiation in the millimeter-wave range 75–110 GHz in the spectrometer.

Since modern ground-based radio telescopes can work in the atmospheric transparency windows at frequencies of up to 1.5 THz [15], we use backward-wave oscillators by the "Istok" Company which cover frequency range of up to 1400 GHz [16], to provide radio-astronomy studies with accurate laboratory measurements of the frequencies of various molecular lines. Both packaged BWOs housed in a magnet and BWOs requiring an external magnetic field are used. For nonpackaged BWOs, electromagnets or permanent magnets with the field induction of up to 1.2 T are used. The magnets and high-voltage power sources for the BWOs (an output voltage of up to 6 kV and a current up to 50 mA) were manufactured at the Institute of Applied Physics of the Russian Academy of Sciences.

The signal from the spectral absorption line is usually obtained by the modulation method with subsequent demodulation of the signal from the radiation detector using an SR830 synchronous amplifier [17]). To measure the absolute values of the absorption coefficient and uniform broadening due to pressure , the amplitude modulation ensured by the mechanical interrupter is used, while the phase modulation is usually used in the problem of accurate estimation of the line centers by the Lamb-dip method to increase the signal-to-noise ratio and the spectral resolution and reduce the interference influence of a signal with uncontrolled radiation entering the detector. A phase modulator similar to that used in [18] (manufactured at the Institute of Applied Physics of the Russian Academy of Sciences) ensures direct modulation of the rubidium-standard signals with frequencies of 5 and 10 MHz (GPS-12RG and SChV-74, respectively), which is a driving reference oscillator for the frequency synthesizer.

Figure 1 shows the block diagram of a spectrometer with the BWO phase-stabilization system. The BWO-signal coherence is ensured by the BWO phase-lock loop (PLL) (manufactured at the Institute of Applied Physics of the Russian Academy of Sciences; see [19] and the literature therein) using the frequency harmonics of the output signal from the multiplying circuit of the PTS-6400 reference synthesizer. The BWO output radiation frequency, its absolute accuracy, and stability depend on the rubidium frequency standard accuracy and stability. The certified long-term frequency stability of the standard amounts to $\Delta\nu/\nu \approx (1–3)\cdot 10^{-12}$, but, its short-term stability for several minutes (typical time of the line measurement) is worse and amounts to $(2–5)\cdot 10^{-10}$ according to our measurements of mutual instability of various rubidium standards. The phase modulator with a frequency of 35 MHz [18] allowed us to modulate the BWO frequency inside the PLL.

The output signal of the PTS-6400 synthesizer is formed by the system of direct digital synthesis (DDS) of frequency, which ensures rapid radiation-frequency tuning with the phase preservation. However, this signal has a rather wide spectral pedestal (about 1 GHz) and weak spurious subharmonics of the fundamental frequency. After the frequency multiplication circuit and the mixer, which is used for the

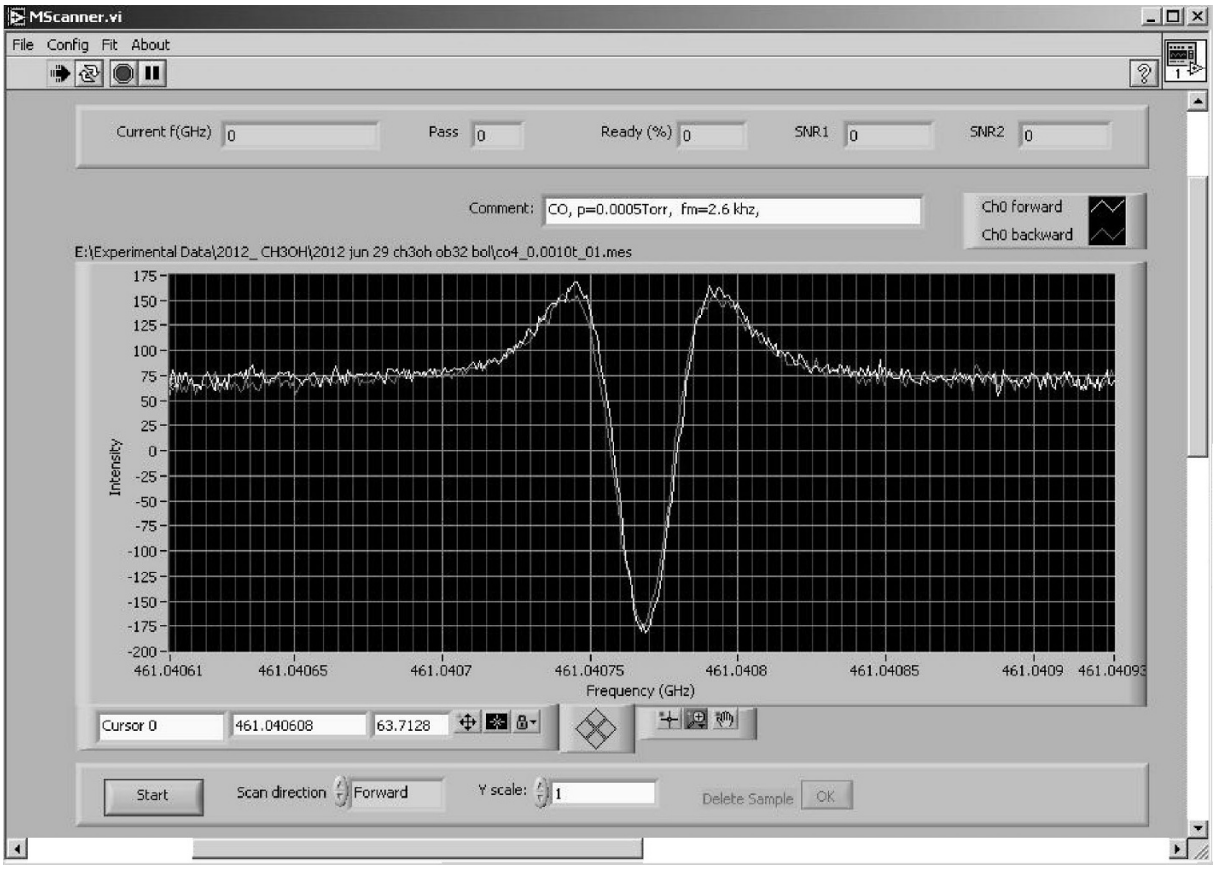

Fig. 2. Lamb dip for the rotational transition $J = 4 \leftarrow 3$ of the $^{12}C\,^{16}O$ molecule, which was recorded during the upward and downward frequency tuning (LabVIEW interface). The averaged line-center frequency is 461040.7688 MHz. The frequency shift of the curves is due to nonzero averaging time of the spectrometer receiver system.

BWO stabilization, the spurious-signal level increases, which significantly deteriorates the PLL operation. Therefore, additional filtering of the output from the signal PTS-6400 synthesizer is performed in the spectrometer using an FFLK2-17 tunable bandpass ferrite filter by the "Zavod Magnetron" Company with the passband 12–60 MHz.

The measurements show that sensitivity with respect to the absorption coefficient of the spectrometer with the InSb hot-electron bolometer by QMC Company (model QFI/2) was of the order of 10^{-8} cm^{-1} for $T = 4.2$ K and 10^{-7} cm^{-1} for the Schottky diode receiver in the millimeter-wave range at room temperature. Sensitivity of the Schottky diode receiver drastically deteriorated with increasing radiation frequency. The spectrometer sensitivity was measured using the carbon-monoxide isotopologues $^{12}C^{16}O$, $^{13}C^{16}O$, $^{12}C^{17}O$, and $^{13}C^{18}O$ in natural concentration.

Tuning the PTS-6400 synthesizer frequency and digitizing the receiver signal from the spectral gas lines are performed using a computer with the GPIB communication card and the National Instruments data-acquisition board. The control and data-acquisition graphics code was written in the LabVIEW environment. Figure 2 shows the LabVIEW graphics interface and an example of the record of the CO line $J = 4 \leftarrow 3$.

3. SPECTRAL-LINE MEASUREMENT ACCURACY

Figure 3 shows the Lamb-dip record for the rotational transition $J = 9 \leftarrow 8$ of the OCS molecule in the form of the second derivative of the line profile, which is obtained using the signal phase modulation and demodulation at the second harmonic of the modulation-frequency harmonic. Fitting the experimental result together with the Voigt frequency profile (solid line) determined the line-center frequency as 109

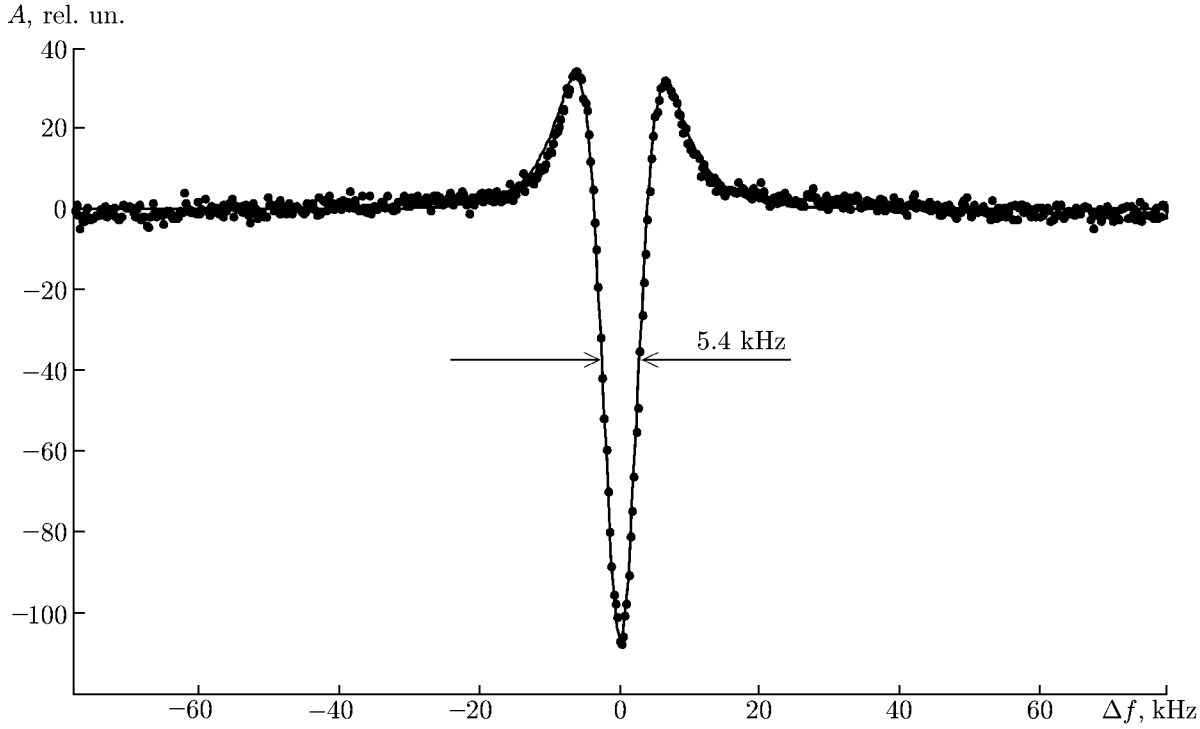

Fig. 3. Lamb-dip record (dots) for the rotational transition $J = 9 \leftarrow 8$ of the OCS molecule. Detuning Δf from the frequency 109 463.064 Mhz is on the horizontal axis and the received-signal amplitude A is on the vertical axis. The solid line shows the result of fitting the experimental data together with the Voigt frequency profile. The actual Lorentz-line half width at half maximum is equal to 6.56(3) kHz.

463.0638(3) MHz (the tabulated value is 109 463.0631(1) MHz [10]) with a halfwidth of 6.56(3) kHz at a half maximum of the line. Since the line-center estimation accuracy and the spectrometer resolution are important to us, the measurement regime (Fig. 3) is chosen such that the Lamb-dip line is obtained with a minimum possible width and a large signal-to-noise ratio (SNR).

The molecule collision with the walls of the spectrometer absorbing cell because of the thermal motion of the molecules is one of the causes of the Lamb-dip broadening. For the cell radius $R = 5.6$ cm and room temperature $T = 298$ K, this broadening according to [20] (half width at half maximum of the Lorentz line, which amounts to $\Delta\nu_{\rm c} \approx (2\pi)^{-1}\,(2R)^{-1}\,V_{\rm m}$, where $V_{\rm m} = (2kT/M)^{1/2}$ is the velocity of a molecule with mass M, and k is Boltzmann's constant) does not exceed 1 kHz for most molecules. The finite time of the molecule interaction with the spatially inhomogeneous field of an electromagnetic wave is the other and basic broadening mechanism. For the beam with the Gaussian intensity distribution of radiation across the cell radius, the above broadening amounts to $\delta\nu \approx 0.4V_{\rm m}/w$ [3], where w is the Gaussian-beam radius. In our case, the beam radius is restricted by the transverse cell size. Therefore, $\delta\nu \approx 6$ kHz for the CO molecule at room temperature. The narrower Lamb dips for the molecules with commensurable masses cannot be obtained without increasing the diameter of the spectrometer cell or its cooling [5].

The standing-wave phase-front distortion because of the beam divergence and multimode nature, as well as noncollinearity of the direct and reflected rays, leads to the depth decrease and additional broadening of the saturation line. Unfortunately, it is difficult to control the radiation phase-front quality of the millimeter and submillimeter waves in a spectrometer cell.

Another broadening effect of a uniform spectral line, namely, broadening because of the transition saturation due to the high radiation intensity, can be estimated by the formula $\Delta\nu_E[\text{kHz}] = 437d[\text{D}] \times (W[\text{mW/cm}^2])^{1/2}$, where $\Delta\nu_E$ is the Rabi frequency [3], d is the dipole moment of the spectral molecule transition, and W is the radiation-energy flux density. The value of $\Delta\nu_E$ is about 5 kHz for the CO molecule

($d = 0.11$ D) for the radiation power 1 mW and the effective beam radius 3 cm. A decrease in the beam-energy flux density leads not only to the line narrowing, but also to the dip-depth decrease, and, therefore, to the SNR decrease. The optimal density of the radiation-energy flux in the cell is chosen using the correcting lens and the wire grid polarizer which is used as an attenuator (Fig. 1).

Using the modulation principle for detecting the line also leads to additional line-profile broadening and distortion. If the phase (frequency) modulation is used when the frequency deviation δ and the modulation frequency f_m are smaller than the Lorentz half width $\Delta\nu$ of the line, then the line profile is distorted only slightly [21]. To record the line, the first or second modulation-frequency harmonics is usually used such that the recorded signal takes the form of the first or second derivative of the line shape. To obtain the maximum SNR, the frequency deviation and the modulation frequency should take the values $\delta \approx 2.2\,\Delta\nu$ [22]. In this case, the modulation broadening is proportional to $\Delta\nu$, which deteriorates the spectrometer resolution by a factor of two.

Since the collisional broadening of the molecule lines is directly proportional to the gas pressure and usually amounts to 3–20 kHz/mTorr, depending on the molecule type (about 3 kHz/mTorr and 6 kHz/mTorr for the CO and OCS molecules, respectively), the spectrometer cell pressure should not exceed 1 mTorr and noticeably vary during the measurement (5–10 min) to obtain narrow Lamb dips. The measurements show that the cell structure ensures conditions which are required for obtaining and measuring the Lamb dip, i.e., the cell is pumped out to 10^{-6} Torr and the rate of atmospheric-gas infiltration onto the cell does not exceed 0.5 mTorr/h.

As is evident from the above discussion, the difficulty of obtaining narrow Lamb dips is that it is necessary to decrease the gas pressure in the cell, modulation frequency, frequency deviation, and the radiation-energy flux, which reduces the received-signal power and the SNR. The Lamb-dip record shown in Fig. 3 for the rotational transition $J = 9 \leftarrow 8$ of the OCS molecule demonstrates minimum nonlinear-resonance width which is close to the limiting value for this spectrometer.

For a single profile record, the error of the line-center frequency measurement is determined by the relation $\Delta\nu/(\mathrm{SNR} \cdot N^{1/2})$ [23], where N is the number of the digital-record dots on the line width. For the line $J = 9 \leftarrow 8$ of the OCS molecule in Fig. 3, the line-center frequency determination error resulting from processing the entire experimental-data file is only about 30 Hz. The systematic error in determining the line-center frequency, which is due to nonzero constant of the receiving-system averaging time, is ruled out by recording the signal during the upward and downward frequency tuning at identical rates (see Fig. 2) and independent processing of each path. The unbiased line-center frequency is determined as the mean value of these measurements.

Nevertheless, the actual line-center measurement error, which is determined from several records, can appear much larger. As an example, Fig. 4 shows the Lamb-dip record at the rotational transition $J = 3 \leftarrow 2$ of the CO molecule, while Fig. 5 demonstrates the results of numerous measurements of the corresponding line. One of the causes of the spread is related to the frequency dependence of the standing-wave amplitude in the spectrometer cell and the spurious-radiation flux entering on the detector, which leads to the "apparent" deviation of response-center frequency from the line and the systematic measurement error of the absorption-line center frequency. Although the line record in the form of the second derivative reduces the frequency-determination error, this type of systematic error cannot be completely ruled out because of the reflections from the elements of the quasioptical channel of the spectrometer. The measurements show that for this reason, the apparent deviation of the isolated-line frequency on the average is from one to several kilohertz. Therefore, to measure the line frequencies with a higher accuracy, one should vary the frequency dependence of the flux arriving at the radiation detector by a slight displacement of the reflector or another optical element of the spectrometer and average the measured results after obtaining the maximum and minimum values of the Lamb-dip center frequency (see [10, 24]).

It should be noted that the measurement data in Fig. 5 are obtained on different days with three different reference synthesizers in the spectrometer and different PLL configurations. Statistical spread of the line-center measurements over 38 measurements (Fig. 5) amounts to 340 Hz, which significantly exceeds

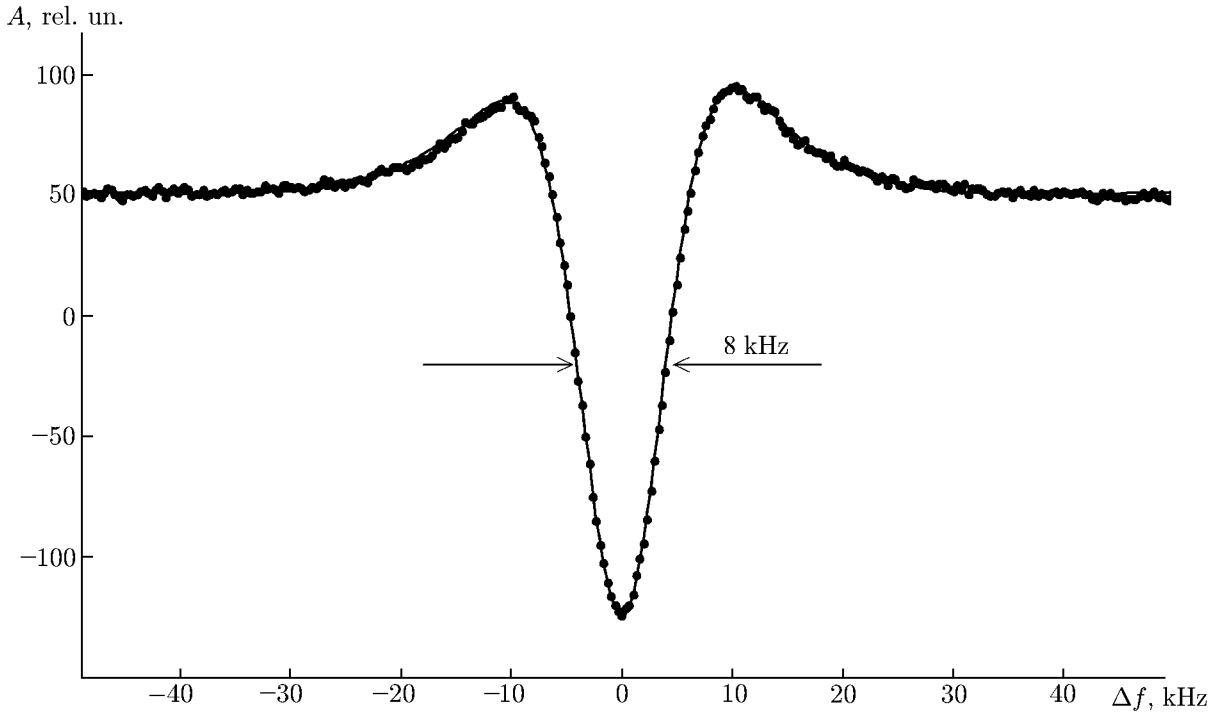

Fig. 4. Lamb-dip record (dots) for the rotational CO transition $J = 3 \leftarrow 2$.

the line-frequency determination error 25 Hz on the basis of one measurement (Fig. 4). The mean transition frequency averaged over all measurements is equal to 345795990.50(34) kHz and somewhat differs from the previous values: 345795991(1) kHz [24], 345795989.8(4) kHz [10], and 345795989.9(5) kHz [25]. The spread of all measurement results is within 1 kHz. This procedure allows us to estimate a possible systematic measurement error, but requires considerable time.

Table 1 shows the results of the measurements of the rotational transitions of the OCS molecule, which were performed using this spectrometer, and comparison with the previous measurements and calculated values [10]. The frequency f measured in this work is given in the second column of Table 1, frequency $f_{[10]}$ measured in [10] is given in the second column, the calculated value of $f^{\mathrm{p}}_{[10]}$ according to [10] is given in the fourth column, and the difference between the measured (in this work) and calculated (according to [10]) frequency values is given in the fifth column. Table 1 shows a small systematic discrepancy among the frequencies. This discrepancy indicates the problem of revealing the systematic measurement error, which can exceed the accuracy of the line-center determination by mathematical processing of the experimental data for the chosen line-profile model. In our opinion, the accuracy of determining the center frequencies of the lines of the OCS-molecule rotational transitions in this work is higher than in [10].

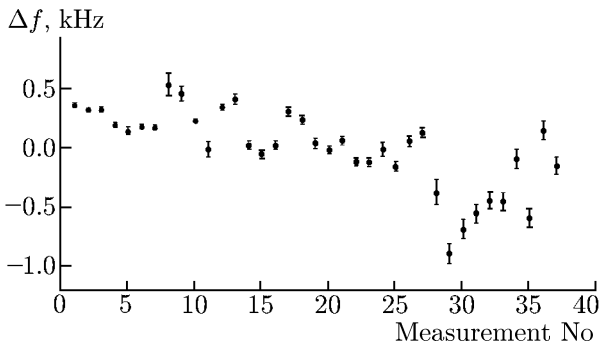

Fig. 5. Measurements of the line center for the rotational transition $J = 3 \leftarrow 2$ of the CO molecule. The transition frequency averaged over all measurements is equal to 345795990.5 ± 0.34 kHz.

Many lines have hyperfine structure due to quadrupole, spin-rotational, and spin–spin interactions in the molecule. If molecular transitions inside the Doppler profile have common energy levels, then additional phantom lines $C_{i,j}$ (or cross resonances) along with the actual transitions are recorded by the Lamb-dip method. The subscripts for the phantom lines denote the level index, e.g., $E_{i,j} = (E_i + E_j)/2$ (where E_i and E_j are the energies of the corresponding actual levels). This effect can either improve the line-center

TABLE 1. Measured and calculated frequencies of the rotational-transition frequency of the molecule $^{16}O^{12}C^{32}S$.

transition $J+1 \leftarrow J$	f, MHz	$f_{[10]}$, MHz	$f^{\mathrm{p}}_{[10]}$, MHz	$f - f^{\mathrm{p}}_{[10]}$, kHz
$4 \leftarrow 3$	48651.60334(198)	48651.603(1)	48651.60375(4)	−0.41
$7 \leftarrow 6$	85139.10521(54)	85139.1032(7)	85139.10404(07)	1.17
$8 \leftarrow 7$	97301.20897(26)	97301.20849(12)	97301.20850(8)	0.47
$9 \leftarrow 8$	109463.06386(17)	109463.063(5)	109463.06308(9)	0.78
$15 \leftarrow 14$	182427.19471(13)	182427.1956(20)	182427.19377(12)	0.94
$19 \leftarrow 18$	231060.99381(40)	231060.9934(13)	231060.99308(13)	0.73
$20 \leftarrow 19$	243218.03780(33)	243218.0364(14)	243218.03720(13)	0.60
$21 \leftarrow 20$	255374.45714(51)	255374.4558(13)	255374.45656(13)	0.58
$22 \leftarrow 21$	267530.22052(52)	267530.2190(14)	267530.21990(13)	0.62
$23 \leftarrow 22$	279685.29666(59)	279685.2958(21)	279685.29597(14)	0.69
$24 \leftarrow 23$	291839.65362(80)	291839.6532(10)	291839.65352(14)	0.11
$25 \leftarrow 24$	303993.26239(32)	303993.2617(11)	303993.26130(14)	1.09
$26 \leftarrow 25$	316146.08863(74)	316146.0890(12)	316146.08805(14)	0.61
$27 \leftarrow 26$	328298.10266(94)	328298.1025(10)	328298.10253(14)	0.13
$28 \leftarrow 27$	340449.27391(82)	340449.2733(8)	340449.27347(15)	0.44
$29 \leftarrow 28$	352599.57022(39)	352599.5703(12)	352599.56961(15)	0.61
$30 \leftarrow 29$	364748.96032(47)	364748.9586(13)	364748.95970(16)	−0.38
$31 \leftarrow 30$	376897.41268(57)	376897.4129(7)	376897.41247(17)	0.21
$32 \leftarrow 31$	—	389044.8976(11)	389044.89666(18)	—
$33 \leftarrow 32$	401191.38104(12)	401191.3811(13)	401191.38101(20)	0.03
$34 \leftarrow 33$	—	413336.8344(10)	413336.83423(21)	—
$35 \leftarrow 34$	425481.22489(23)	425481.2254(8)	425481.22507(23)	−0.18
$36 \leftarrow 35$	—	437624.5221(7)	437624.52225(25)	—
$37 \leftarrow 36$	—	449766.6936(14)	449766.69450(28)	—
$38 \leftarrow 37$	461907.71040(38)	461907.7107(10)	461907.71053(30)	−0.13
$39 \leftarrow 38$	—	474047.5375(20)	474047.53908(32)	—
$40 \leftarrow 39$	—	486186.1479(23)	486186.14885(35)	—
$41 \leftarrow 40$	498323.50802(54)	—	498323.50857(38)	−0.55
$42 \leftarrow 41$	510459.58671(109)	—	510459.58694(41)	−0.23
$43 \leftarrow 42$	522594.35135(117)	—	522594.35267(44)	−1.32

determination accuracy, provided the lines are well resolved, or lead to the line overlapping [26, 27], which significantly impedes the molecule-transition identification.

To check the actual spectrometer resolution, the hyperfine structure of some molecule transitions was measured. For example, we repeated the measurements of the well-known magnetic hyperfine structure of some water-molecule transitions in orthomodification (the total molecule spin is 1), which were performed in [12] and later by an Italian group in [28] with a higher resolution. Figure 6 shows the record of the transition $4_{1,4} \leftarrow 3_{2,1}$ of the water molecule $H_2{}^{16}O$ under a pressure of about 10^{-4} Torr (the natural broadening of the line is 20 kHz/mTorr and the natural shift is 0.3 kHz/mTorr [29]), from which, one can estimate that in the case considered, the spectral resolution of the spectrometer is about 10 kHz.

Apart from the strongest lines of the magnetic hyperfine structure $F' \leftarrow F''$ with the selection rules $\Delta F = 1 : 5 \leftarrow 4$ (380197.332 MHz), $4 \leftarrow 3$ (380197.347 MHz), and $3 \leftarrow 2$ (380197.403 MHz), the phantom lines (Fig. 6) of the corresponding transitions $C_{4,3} \leftarrow C_{3,3}$ (380197.426 MHz) and $C_{3,3} \leftarrow C_{3,2}$ (380197.452 MHz) are also observed. Observation of the less intense transitions $4 \leftarrow 4$ and $3 \leftarrow 3$, which

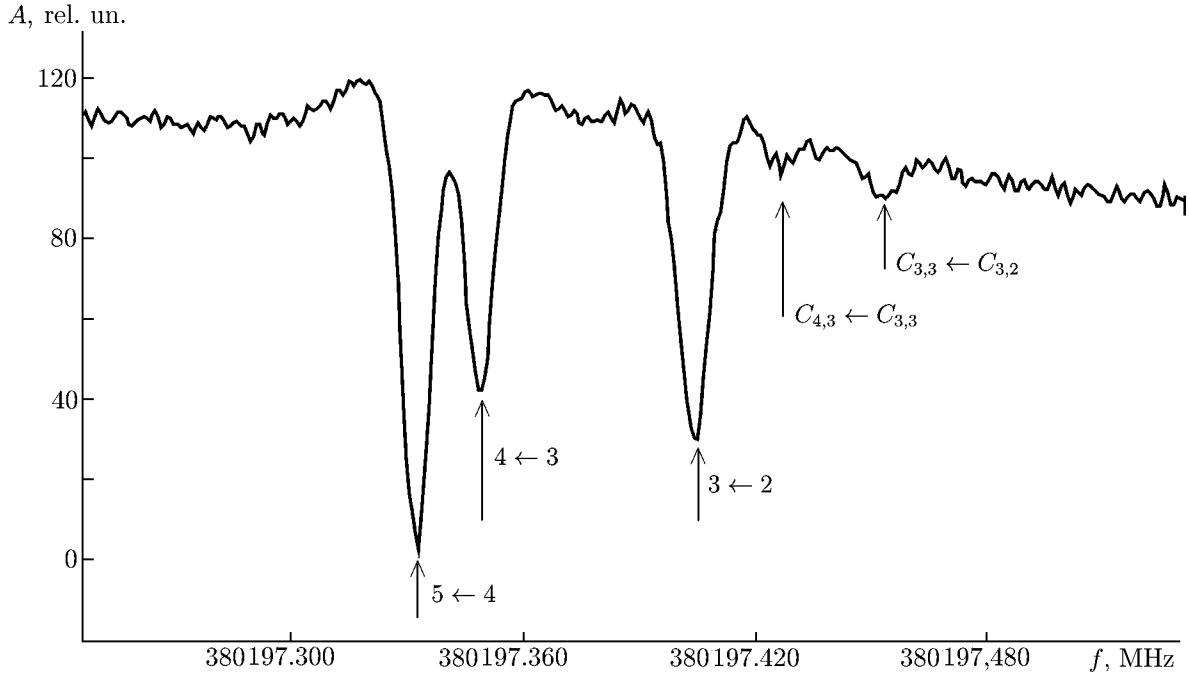

Fig. 6. Record of the magnetic hyperfine structure $F' \leftarrow F''$ of the transition $4_{1.4} \leftarrow 3_{2.1}$ of the $H_2^{16}O$ molecule inside the Doppler profile. The phantom lines which were not previously observed are denoted as $C_{4.3} \leftarrow C_{3.3}$ and $C_{3.3} \leftarrow C_{3.2}$.

TABLE 2. Constants of hyperfine splitting of the water isotopologues.

	C_{aa}(H), kHz	C_{bb}(H), kHz	C_{cc}(H), kHz	$1.5D_{aa}$(H-H), kHz
$H_2{}^{16}O$ [28]	−35.05(25)	−31.02(25)	−32.99(9)	−101.3(22)
$H_2{}^{17}O$ [26]	−34.45(19)	−31.03(19)	−32.91(10)	−100.7(24)
$H_2{}^{16}O$	−34.7(4)	−31.1(3)	−32.9(3)	−103.73
$H_2{}^{18}O$, $1.5D_{aa}$ = const	−35.0(7)	−33.4(7)	−35.2(7)	−101.3
$H_2{}^{18}O$	−33.1(7)	−31.6(7)	−33.8(7)	−104.7(8)

were more than an order of magnitude weaker than those depicted in the figure, is difficult in this case. Line $3 \leftarrow 4$ is weaker by three orders of magnitude. However, using the phantom lines whose intensity is higher, one can determine the frequency of the nonobserved transition $3 \leftarrow 3$, which coincides with the calculated frequency 380197.502(1) MHz. The phantom line $C_{4,5} \leftarrow C_{4,4}$ (380197.404 MHz) coincides with the line $3 \leftarrow 2$, while the line $C_{4,4} \leftarrow C_{4,3}$ (380197.412 MHz) is on the slope in the wing of the same. Therefore, they are not observed, just slightly distorting the line $3 \leftarrow 2$.

We have also measured once again the frequencies of the hyperfine structure of the $H_2{}^{18}O$ molecule (these measurements were performed at the Department of Engineering of the Christian-Albrechts-Universität zu Kiel, Germany). Due to an increase in the spectrometer resolution, we identified the corresponding transitions (resolution is similar to that in Fig. 6) and improved the accuracy of the center-frequency determination compared with the measured results [12], when the value of splitting of the $H_2^{18}O$ component was shifted because of the apparent-shift effect for the closely located lines measured by the frequency-modulation method.

Table 2 presents the constants of the tensor of the magnetic structure of the water isotopologues $H_2{}^{16}O$, $H_2{}^{18}O$, and $H_2{}^{17}O$, which were obtained in this work and in [26, 28], where a higher frequency resolution compared with our previous 2006 measurements [12] was obtained. The constants were calculated using the Pickett's SPFIT code [30]. In our calculations, the spin–spin interaction constant $1.5D_{aa}$ for the

$H_2^{16}O$ molecule was chosen with allowance for the molecule geometry and had a fixed value. The constant $1.5D_{aa}$ for the $H_2{}^{18}O$ molecule either had a fixed value, which was given in [28] (the first line), or remained free (the fifth line). Comparing the two last lines in Table 2 for the $H_2{}^{18}O$ molecule, we should mention correlation between the parameter D_{aa} and the spin-rotational interaction constants C_K, which is also explained by a smaller number of the measured lines for $H_2{}^{18}O$ [12] compared with $H_2{}^{16}O$. It is unclear whether the constant $1.5D_{aa}$ should be assumed equal to the calculated value or remain free for the fitting calculations with allowance for the fact that the water molecule is not rigid. Nevertheless, according to Table 2, it can be stated that the hyperfine-splitting constants almost coincide for all water isotopologues $H_2{}^{16}O$, $H_2{}^{18}O$, and $H_2{}^{17}O$.

4. CONCLUSIONS

The precision sub-Doppler millimeter- and submillimeter-wave spectrometer on the basis of the effect of nonlinear saturation of the molecule spectral transitions by radiation (Lamb-dip method) has been developed. The accuracy of measuring the absolute frequencies of the molecular transitions, which is better than 1 kHz, and a resolution of about 10 kHz in the frequency range below 0.5 THz have been reached. The obtained spectrometer parameters are in line with the modern requirements to providing accurate experimental data for the studies in the radio-astronomy and molecular-spectroscopy fields, as well as fundamental astrophysical investigations. The frequency records of the spectral lines of the CO, OCS, and $H_2^{16}O$ molecules have been demonstrated. The frequencies of the OCS-molecule rotational transitions have been determined up to an accuracy better than 1 kHz and can be the secondary frequency standard. The constants of the tensor of the molecule magnetic structure have been calculated for the $H_2^{16}O$ and $H_2^{18}O$ molecules on the basis of new data.

We sincerely thank I. E. Spektor (Laboratory of Experimental Methods of Submillimeter Spectroscopy at the Institute of General Physics of the Russian Academy of Sciences) for providing wire grid polarizers and A. M. Shchitov (A. P. Gorshkov Research Institute of Electronic Measurements "KVARZ") and V. A. Mal'tsev (Institute of Applied Physics of the Russian Academy of Sciences) for assistance in the design and adjustment of the microwave channel of the reference synthesizer.

This work was financially supported by the Russian Foundation for Basic Research (project Nos. 11–02–00435-a, 09–02–91343-NNIO_a, 13–02–12220-ofi-m, and 12–02–00059-a), the Program "Modern Problems of Radiophysics" of the Branch of Radiophysical Sciences of the Russian Academy of Sciences, and the Ministry of Education and Science of the Russian Federation (contract No. 8421 in the direction "Physics and Astronomy"). The frequency of the $H_2^{18}O$-molecule hyperfine structure was measured with support of the grant DFG-Geschaeftszeichen: KN 253/9-1.

REFERENCES

1. S. A. Levshakov, M. G. Kozlov, and D. Reimers, *Astrophys. J.*, **738**, 26 (2011).
2. A. V. Lapinov, S. A. Levshakov, M. G. Kozlov, et al., *Vestn. RFFI*, No. 1 (73), 111 (2012).
3. W. Demtröder, *Laser Spectroscopy: Basic Concepts and Instrumentation*, Springer-Verlag, Berlin–Heidellberg (2003).
4. V. S. Letokhov and V. P. Chebotaev, *Sov. Phys. Uspekhi*, **17**, No. 4, 467 (1975).
5. V. S. Letokhov and V. P. Chebotaev, *Nonlinear Superhigh-Resolution Laser Spectroscopy* [in Russian], Nauka, Moscow (1990).
6. C. C. Costain, *Can. J. Phys.*, **47**, 2431 (1969).
7. Yu. A. Dryagin, *Radiophys. Quantum Electron.*, **13**, No. 1, 107 (1970).
8. G. Winnewisser, S. P. Belov, Th. Klaus, and R. Schieder, *J. Mol. Spectrosc.*, **184**, 468 (1997).

9. G. Cazzoli, C. Puzzarini, and A. V. Lapinov, *Astrophys. J.*, **592**, L95 (2003).
10. G. Yu. Golubiatnikov, A. V. Lapinov, A. Guarnieri, and R. Knöchel, *J. Mol. Spectrosc.*, **234**, 190 (2005).
11. A. V. Lapinov, G. Yu. Golubiatnikov, V. N. Markov, and A. Guarnieri, *Astron. Lett.*, **33**, No. 2, 121 (2007).
12. G. Yu. Golubiatnikov, V. N. Markov, A. Guarnieri, and R. Knöchel, *J. Mol. Spectrosc.*, **240**, 251 (2006).
13. E. V. Baklanov and V. P. Chebotaev, *Sov. Phys. JETP*, **33**, No. 2, 300 (1971).
14. V. P. Kochanov, S. G. Rautian, and A. M. Shalagin, *Sov. Phys. JETP*, **45**, No. 4, 714 (1977).
15. M. C. Wiedner, G. Wieching, F. Bielau, et al., *Astron. Astrophys.*, **454**, L33 (2006).
16. www.istokmw.ru/vakuumnie-generatori-maloy-moshnosti .
17. www.thinksrs.com .
18. J. Doose, A. Guarnieri, W. Neustock, et al., *Z. Naturforsch. A*, **44**, 538 (1989).
19. A. F. Krupnov, M. Yu. Tretyakov, S. P. Belov, et al., *J. Mol. Spectrosc.*, **280**, 110 (2012).
20. M. Danos and S. Geschwind, *Phys. Rev.*, **91**, No. 5, 1159 (1953).
21. R. Karplus, *Phys. Rev.*, **73**, No. 9, 1027 (1948).
22. J. Reid and D. Labrie, *Appl. Phys. B*, **26**, 203 (1981).
23. D. A. Landman, R. Roussel-Dupre, and G. Tanigawa, *Astrophys. J.*, **261**, 732 (1982).
24. S. P. Belov, M. Yu. Tretyakov, and R. D. Suenram, *Astrophys. J.*, **393**, 848 (1992).
25. G. Winnewisser, S. P. Belov, Th. Klaus, and R. Schieder, *J. Mol. Spectrosc.*, **184**, 468 (1997).
26. C. Puzzarini, G. Cazzoli, M. E. Harding, et al., *J. Chem. Phys.*, **131**, 234304 (2009).
27. G. Cazzoli, L. Dore, C. Puzzarini, and J. Gauss, *Mol. Phys.*, **108**, No. 18, 2335 (2010).
28. G. Cazzoli, C. Puzzarini, M. E. Harding, and J. Gauss, *Chem. Phys. Lett.*, **473**, 21 (2009).
29. M. A. Koshelev, M. Yu. Tretyakov, G. Yu. Golubiatnikov, et al., *J. Mol. Spectrosc.*, **241**, 101 (2007).
30. http://spec.jpl.nasa.gov .